In vitro models
https://doi.org/10.1007/s44164-025-00089-4

ORIGINAL RESEARCH

Multicellular hepatic in vitro models using NANOSTACKS™: human-relevant models for drug response prediction

Abdullah C. Talari[1] · Raffaello Sbordoni[1] · Valmira Hoti[1] · Talha Jalil[1] · Imran I. Patel[1] · Francis L. Martin[1] · Ahtasham Raza[1] · Valon Llabjani[1]

Received: 14 March 2025 / Revised: 2 May 2025 / Accepted: 5 May 2025

Abstract
Drug-induced liver injury (DILI) continues to be one of the leading causes of drug attrition during clinical trials, as well as the number one cause of post-market drug withdrawal due to the limited predictive accuracy of preclinical animals and conventional in vitro models. In this study, the NANOSTACKS™ platform was introduced as a novel in vitro tool to build in vivo-relevant organ models for predicting drug responses. In particular, hepatic models, including monocultures of primary human hepatocytes (PHH), tricultures of PHH, human stellate cells (HSC), and human liver endothelial cells (LECs), and tetracultures of PHH, HSC, LECs, and human Kupffer cells (KC) were developed under static and orbital-induced mixing flow conditions. All hepatic models were characterised by assessing albumin, urea, CYP3A4, and ATP production. In addition, the preclinical DILI screening potential of the orbital-induced mixing flow monoculture and triculture models was assessed by testing the hepatotoxicity of zileuton, buspirone, and cyclophosphamide. NANOSTACKS™ represents a promising tool for the development of complex in vitro models.

Keywords NANOSTACKS™ · Drug-induced liver injury (DILI) · Hepatic models · Complex in vitro models

Introduction

Drug-induced liver injury (DILI) represents a relatively rare yet significant source of acute and chronic liver disease [1]. It is one of the most common causes of post-market drug withdrawal [2]. The detection of hepatotoxicity usually occurs during clinical trials or after a product has been released to the market, leading to elevated hazards for clinical trial participants and imposing huge financial strains on drug development research [3]. One of the reasons underlying failures in drug development arises from the limited predictive accuracy of preclinical models [4], which involve animal models and conventional in vitro models.

Animal models are used for assessing DILI and evaluating pharmacokinetics despite their inter-species differences with humans with regard to physiology, genetics, and drug metabolism [5]. A comprehensive large-scale study comparing the effectiveness of animal models in detecting DILI in humans indicated poor predictive performance [6]. Among the 150 hepatotoxins studied, both rodent and non-rodent models were only able to detect 50% of the human hepatotoxic events associated with these drugs [6]. To address this issue, in vitro models replicating aspects of human hepatic biology could be utilised.

Most liver in vitro models adopted to screen DILI toxicity are typically based on 2D liver monoculture cell models. Nevertheless, these models are primarily constrained by their lack of crosstalk between different cell types, inconsistent findings with regard to the prediction of hepatotoxicity, and lack of tissue-like organisation; such factors are essential for establishing a liver model that accurately mimics physiological conditions [7]. Recently, the US Food and Drug Administration (FDA) Modernization Act 2.0 has highlighted the need for alternatives to animal testing and to traditional in vitro models, such as 3D in vitro models based on the use of organoids and microphysiological systems [8]. In the context of hepatotoxicity assessment, alternatives to traditional in vitro models include sandwich-cultured hepatic cells, whole organ explants, precision-cut tissue slices, tumour tissue explants, hepatic spheroids, organoids, and liver models developed using microfluidic systems [9–13].

✉ Valon Llabjani
valon@revivocell.com

[1] Sci-Tech Daresbury, REVIVOCELL Limited, Keckwick Lane, Daresbury, Warrington WA4 4 AD, UK

Published online: 18 June 2025

In comparison to traditional in vitro models, these advanced models can simulate and predict cellular behaviour and therapeutic responses with higher reliability [14, 15].

The type of cells included in the in vitro model also plays a key role in determining its capability to predict hepatotoxicity. The human liver consists of two main types of cells: hepatocytes and non-parenchymal cells (NPC). NPCs include liver endothelial cells, stellate cells and Kupffer cells [16]. Primary human hepatocytes (PHH) widely regarded as the "gold standard" for in vitro drug testing. Over the past two decades, they have been extensively used in toxicological and pharmacological studies [17, 18].

In the context of preclinical in vitro screening models, preserving the metabolic function of PHH over an extended period of cell culture is a significant focus. Interactions between hepatocytes and non-parenchymal cells (NPCs) can significantly influence metabolic activity and toxicological responses, which are essential for accurately assessing hepatic safety mechanisms [16]. Hepatocytes cocultured with stellate cells display improved physiological and metabolic functions, and their hepatic function is better maintained [19]. For instance, PHH cocultured with stellate cells exhibits a more stable liver phenotype compared to monocultures [20–22]. Similarly, the coculture of hepatocytes with liver endothelial cells in a microfabricated perfusion reactor resulted in the formation of endothelial network structures and high retention of hepatocellular function compared to monocultures [23]. Various other cellular combinations involving PHH have been investigated, including the use of NIH/3 T3 [24, 25], endothelial cells [26, 27], and Kupffer cells [28, 29].

In order to set up a coculture model, a common approach is to mix different cell types in a single well [30, 31]. The mixture approach offers the advantage of facilitating direct cell–cell contact, allowing the evaluation of interactions mediated by cell adhesion. However, this method does not replicate the layered microarchitecture of hepatic lobules. Another approach is that cultivating primary human hepatocytes (PHH) in a three-dimensional (3D) sandwich setup, surrounded by two layers of extracellular matrix (ECM), promotes 3D adherence. This arrangement facilitates the development of cell–cell and cell–matrix interactions resembling those found in vivo [32, 33]. This method models the natural layering of liver cells whilst maintaining constant ratios between the cell numbers of different cell types included in the model. However, the sandwich method is time-consuming, challenging to reproduce, and labour-intensive [34]. Human liver microphysiological systems (MPS) have the potential to address the limitations of current coculture models by utilising engineering and design principles that more accurately replicate human liver physiology in miniatured systems. These advanced models may incorporate various sophisticated features such as a multicellular environment, 3D architecture, and exposure to fluid flow. However, MPS-based models can be complicated to develop and use, therefore reducing their applicability in the context of DILI screening.

To address issues associated with currently used models, in this work NANOSTACKS^{TM} (NS), a novel user-friendly, imaging- and orbital-induced mixing compatible platform, was used for the assembly of complex hepatic cocultures in a 24-well plate format. In particular, hepatic models based on monocultures of PHH, tricultures of PHH, human stellate cells (HSC), human liver endothelial cells (LECs), and tetracultures of PHH, HSC, LECs, and human Kupffer cells (KC) on NS were developed. The models were characterised with regard to parameters associated with hepatic function in the absence or presence of orbital-induced mixing flow. Finally, three different compounds (zileuton, buspirone, and cyclophosphamide) were tested on the triculture and monoculture hepatic models to assess their reliability for preclinical DILI screening.

Methods

Cell culture

Cryopreserved primary human hepatocytes (PHH) (Lot 2211419-01), primary human liver endothelial cells (LECs) (Lot 2211419p0), primary human stellate cells (HSC) (Lot 2216631p0) and primary human Kupffer cells (KC) (Lot 2211419) were purchased from LifeNet Health LifeSciences. This study represents the first application of our patented NANOSTACKS™ platform. To establish a controlled and consistent baseline for evaluating the system's performance, we selected PHH and NPC derived from the same donor. Using cells from the same donor minimises inter-donor variability and reflects the capabilities of the NANOSTACKS™ platform rather than differences between unrelated cell sources. All primary cells were cultured in accordance with the protocols specified by the vendor. Before seeding on NS, both LECs and HSC were expanded on rat collagen type I (Gibco^{TM})-coated T-25 flasks (Fisher Scientific). LECs were expanded using LECs complete medium, composed of Lonza EBM-2 and Lonza EGM-2, whilst HSC were expanded using HSC complete medium, composed of DMEM (Gibco^{TM}), 10% fetal bovine serum (FBS) (Sigma) and 1% Pen/Strep (Sigma). PHH and KC were thawed according to the vendor's protocols on the day of seeding on NS.PHH thawing medium, plating medium and maintenance medium were provided by LifeNet Health LifeSciences. KC complete medium, which was used to culture KC on NS before initiating the tetraculture, was composed of RPMI 1640 (Gibco^{TM}), 10% FBS (Sigma) and 1% Pen/Strep (Sigma).

NANOSTACKS™ (NS) design

NS enable cell culture through their stackable design within a standard SBS 24-well plate format (Fig. 1). In particular, up to four NS can be stacked in a single well, and therefore up to four different cell types can be cocultured within the same in vitro model. The cell culture medium can diffuse across the gaps between each NS. In our experimental design, each cell type was initially seeded onto the NANOSTACKS™ using its respective optimised medium to ensure optimal attachment and viability. However, when the individual cell layers were assembled to form the full model, all cell types were subsequently maintained in a single, common medium—specifically, the PHH maintenance medium supplied by the vendor. Cell-to-cell communication in NS modelling occurs through media-based paracrine signaling, which is a key mechanism facilitating interactions between different cell types. While the NS modelling lacks direct cell-to-cell contact, this platform is intended to serve as a foundation for developing multiple organ models, enabling complex inter-organ communication and functional integration. Additionally, each NS includes a porous membrane with a pore size of 0.4 µm, increasing nutrient diffusion towards cells. Additionally, the porous membrane of NS is transparent, thus allowing live imaging without disrupting the multilayered structure. To avoid material absorption of pharmaceutical compounds, the body of NS is composed of polycarbonate, whilst the membrane is composed of polyester. In order to induce orbital-induced mixing on the NS, the 24-well plates, including the devices, can be placed on an orbital shaker.

Human liver modelling on the NANOSTACKS™ (NS) platform

Three types of human liver models were developed using NS. In particular, the models were a monoculture model (PHH), a triculture model (PHH + LECs + HSC) and a tetraculture model (PHH + LECs + HSC + KC). All the models were developed with and without the inclusion of orbital-induced mixing. Throughout the experiment, NS were kept in wells of 24-well plates. All NS were coated with 10 µg/cm^2 rat collagen type I at RT and then washed thrice using phosphate-buffered saline (PBS). PHH, LECs, HSC, and KC were seeded at a 3:1:1:1 proportion, respectively, to the seeding density of the individual cell type. In particular, a cell seeding suspension volume of 70 µL was decanted on the top surface of the cell culture-treated membrane on each NS, and cells were incubated at 37° and at 5% CO_2 in a humidified incubator for 2 h to allow cell attachment. PBS was added to empty wells of the well-plate to prevent evaporation of the cell suspension droplets. Then, 1430 µL of medium was added to the seeded NS to reach the working volume of 1.5 mL, and subsequently, the plates were left in a cell culture incubator for 24 h. Each cell type was seeded using its respective complete medium.

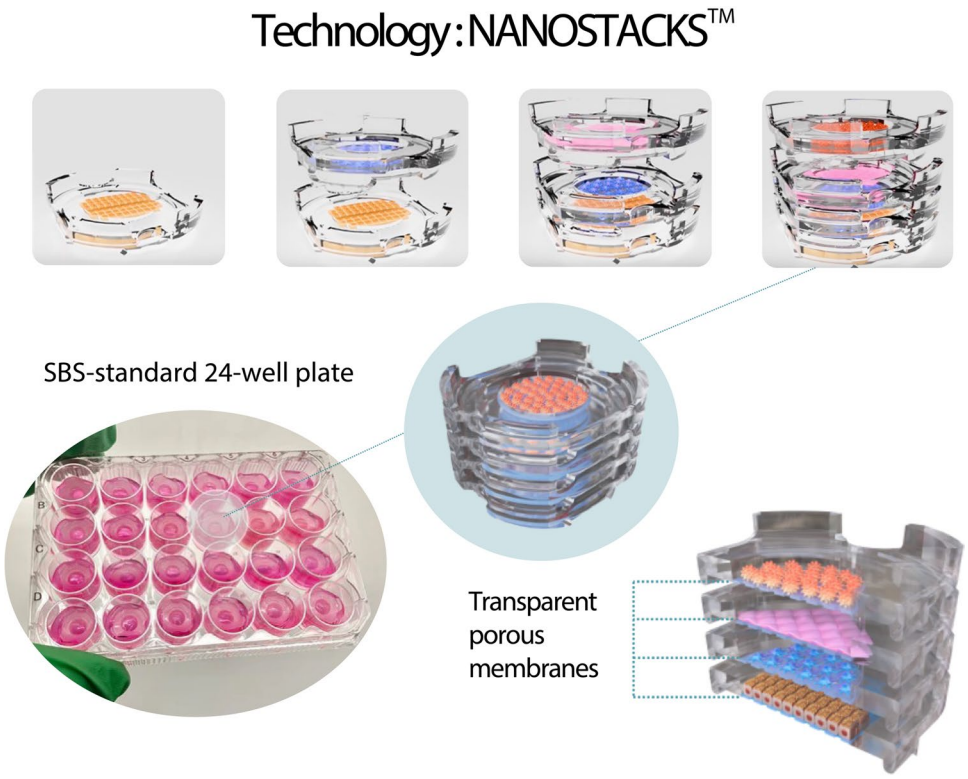

Fig. 1 Graphic representation of the NS platform. Up to four cell-seeded NS can be stacked on top of each other (top), forming a complex coculture (centre) that can be housed into wells of an SBS-standard 24-well plate (bottom-left). Each NS is made of a polycarbonate body and a transparent porous PET membrane with a pore size of 0.4 µm (bottom right). Orbital-induced mixing can be induced by placing the 24-well plate, including the NS, on an orbital shaker

On day 1, each NPC (LECs, HSC, and KC) was seeded at a seeding density of 16.6×10^3 cells/mL, whereas on day 0, PHH were seeded at a seeding density of 50×10^3 cells/mL. On day 1, the in vitro models were assembled by stacking the cell-seeded NS in order to combine the different cell types into monoculture, triculture and tetraculture models (Fig. 2A). In particular, in the monoculture model, one PHH-seeded NS was placed in each well. In the triculture model, one PHH-seeded NS was placed at the bottom of each well, and one HSC-seeded, and one LEC-seeded were placed on top. In the tetraculture model, one PHH-seeded NS was placed in the bottom of each well, and one HSC-seeded, one LECs-seeded, and one KC-seeded NS were placed on top of the PHH-seeded NS. Additionally, for monoculture models, three membrane-free, cell-free NS were added on top of the cell-seeded NS, whilst for triculture models, one membrane-free, cell-free NS was added on top of the three cell-seeded NS, in order to maintain the same height of cell culture medium in the wells of all hepatic models. Once the models were assembled, PHH culture medium was used to maintain the cultures, with medium changes occurring every 2 days. On day 1, each model was assigned either to a static condition or to an orbital-induced mixing condition, the latter entailing the inclusion of orbital-induced mixing by placing the 24-well plate, including the NS, on an orbital shaker (TOS-3530 CO2; Munro Scientific) set at 90 RPM. The rotation was circular, and the orbital shaker with 90 RPM provided gentle and continuous orbital-inducing flow over cell layers, thereby mimicking low shear stress. Monocultures and tricultures were maintained in culture for 31 days, whilst tetracultures were maintained for 26 days. All models underwent characterisation based on cell viability, albumin, urea, and CYP3 A4 metabolic activity measurements. DILI toxicity screening was conducted exclusively on the monoculture and triculture models. Each assay was performed on $n = 3$ wells per timepoint in both static and orbital-induced mixing conditions.

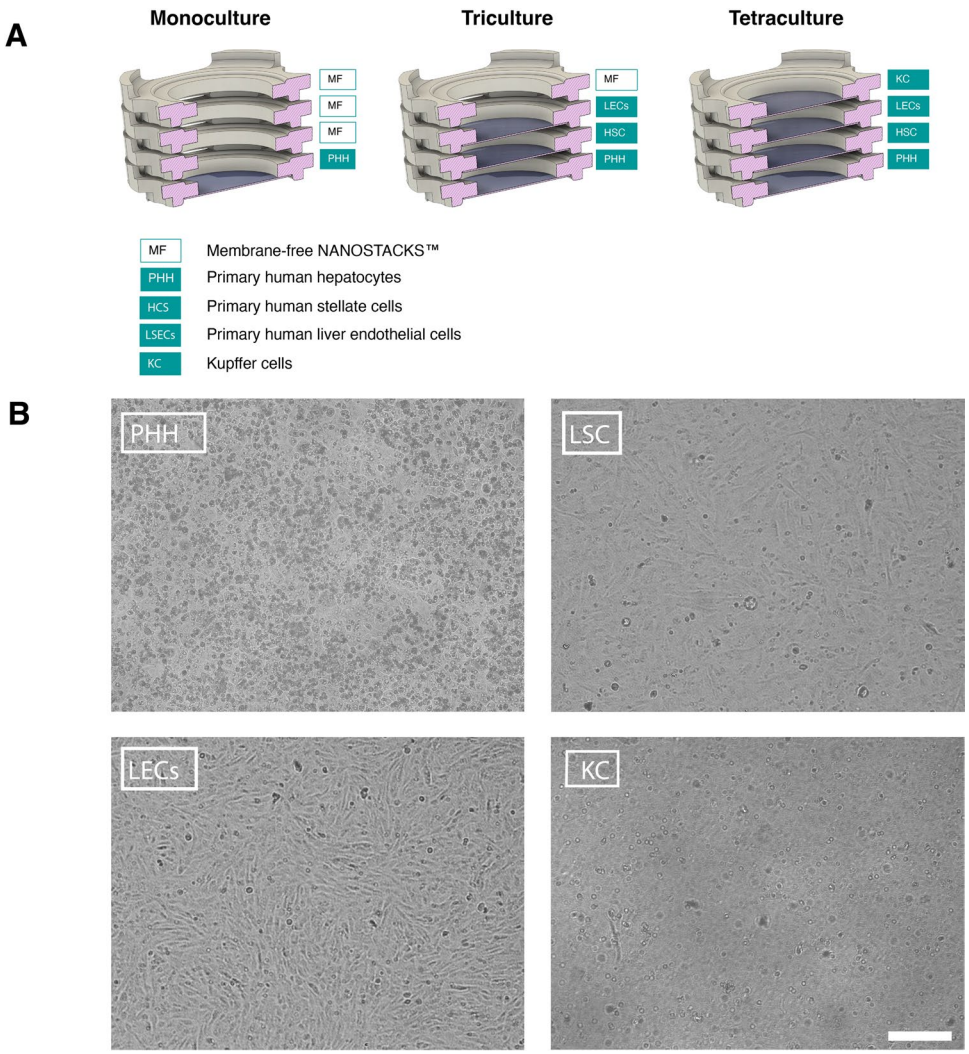

Fig. 2 **A** Schematic representation of the experimental setup. **B** Representative widefield image of primary human hepatocytes (PHH), primary human stellate cells (HSC), primary human liver endothelial cells (LECs), and primary human Kupffer cells (KC) on NS, acquired on day 2. Magnification: × 10. Scale bar: 250 µm

Cell viability

The CellTiter-GLO assay (CellTiter-Glo® Luminescent Cell Viability AssayG7571, Promega), which measures intracellular ATP content as a biomarker of cell viability, was performed according to the protocol provided by the vendor, with the following modifications: cell-seeded NS were moved to wells of a 24-well plate including 350 µL of medium, and then 350 µL CellTiter-GLO reagent was added onto each well to obtain a 1:1 dilution. The luminescence of each well was read by a Synergy H1 Microplate reader (Fisher Scientific) and analysed with the GEN5 software (BioTek; version 2.05). The CellTiter-GLO assay was performed on $n = 3$ wells per timepoint on days 2, 4, 7, 11, 14, 20, 26, and 31.

Cytochrome P450 assay

CYP3 A4 expression in PHH was measured with a P450-GLO assay (V9001 Luciferin-IPA, Promega). The P450-Glo™ assay technology provides a rapid, high-throughput method for assessing cytochrome P450 (CYP) activity by measuring the conversion of inactive D-luciferin derivatives to an active form. The emitted light intensity is directly proportional to the CYP enzyme activity. The assay was performed on days 2, 4, 7, 11, 14, 20, 26, and 31 according to the protocol provided by the vendor on the same NS used for viability analysis. The assay was performed on $n = 3$ wells per timepoint.

Albumin assay

The albumin produced by cells within the liver models was quantified on days 2, 4, 7, 11, 14, and 26 using sandwich ELISA kits (Albumin ab179887, Abcam). In particular, the supernatant obtained from each well was preserved at − 80 °C, then thawed overnight at 4 °C. Subsequently, the supernatant samples were diluted 50-fold with the buffer provided by the vendor, and the assay was performed following the vendor's instructions. In the last step of the assay, absorbance at 450 nm was measured using the Synergy H1 Microplate reader and analysed with the GEN5 software. The assay was performed on $n = 3$ wells per timepoint.

Urea assay

Urea produced by PHH in the liver models was quantified using a urea assay kit (MAK006, Sigma-Aldrich) on days 2, 4, 7, 11, 14, and 26. The supernatant obtained from each well was preserved at − 80 °C and thawed overnight at 4 °C. Subsequently, the supernatant samples were diluted 50-fold with the buffer provided by the vendor. The assay was then performed according to the instructions of the vendor. Finally, absorbance at 570 nm was measured using the Synergy H1 Microplate reader and analysed with the GEN5 software. The assay was performed on $n = 3$ wells per timepoint.

Toxicity screening

The dose–response effects of zileuton, buspirone hydrochloride and cyclophosphamide were assessed at concentrations ranging from 1 to 600 times the human C_{max} on monoculture and triculture models. The experiments were conducted on day 4 on monocultures and on day 7 on tricultures models. The compounds were dissolved in DMSO, which was used at a concentration of 0.1 % V/V in a cell culture medium and was also included as vehicle control. The models were treated with the compounds every day for 7 days. Total cytotoxicity of the compounds was then measured using the CellTiter-Glo® Luminescent Cell Viability Assay (G7571, Promega), as previously described. Drug treatments were performed in $n = 3$ wells per compound and concentration.

Fluid dynamics modelling on NANOSTACKS™

A computational fluid dynamics (CFD) model was developed using the software ANSYS-CFX (ANSYS Inc.) to model the shear stress exerted on NS placed into wells of a 24-well plate in an orbital shaker set at 90 RPM. In particular, CFD modelling was performed on a well including one NS inclusive of membrane (bottom of the well) and three NS without membranes, on three NS inclusive of membranes (bottom of the well) and one NS without membrane, on four NS including membranes, and on an NS-free well. The orbital diameter of the orbital shaker was 19 mm, and the volume of cell culture medium was 1.5 mL in all configurations. The medium was modelled as an incompressible and Newtonian fluid with a dynamic viscosity (µ) of 0.7 mPa·s at 37 °C, and medium density $\rho = 1000$ kg/m^3 as described by Driessen et al. [35].

Statistical analysis

For each timepoint associated with ATP, CYP3 A4, albumin and urea production, unpaired Student T-tests were performed using the software Prism (GraphPad; version 10.2.3) to analyse the differences between the static and orbital-induced mixing conditions. A p-value < 0.05 was assumed to indicate a statistically significant difference, indicated by asterisks in the graphs (*: $p < 0.5$; **: $p < 0.01$; ***: $p < 0.001$; ****: $p < 0.0001$). Values are reported in the graphs as mean ± SEM.

Results

In this work, NS-based monocultures (PHH), tricultures (PHH-HSC-LECs) and tetracultures (PHH-HSC-LECs-KC) liver models were developed under static and orbital-induced mixing conditions; the latter induced by placing the 24-well plate including the NS onto an orbital shaker. To quantify the shear stress exerted on the cell culture surface of the inserts in monoculture and coculture configurations, a computational fluid dynamics (CFD) analysis was performed (Fig. 3). The shear stress was highest on the membrane included in NS occupying the position closest to the air–liquid interface in cocultures (Fig. 3C and 3D), comparatively to other NS membranes positioned closer to the bottom of the well (Fig. 3B–3D). Additionally, the shear stress profile of the NS membrane associated with the monoculture condition (Fig. 3B) was found to be more spatially uniform than the shear stress profile related to the bottom surface of an empty well (Fig. 3A).

NS-based liver models, including PHH monoculture, tricultures, and tetracultures, were consistently maintained in a working volume of 1.5 mL of medium across the NANOSTACKS™ platform. Although the volume is higher than the 500 µL typically used in standard static cultures, we did not observe signs of hypoxic stress, such as reduced viability or loss of hepatocyte-specific functions in the PHH. The NS-based liver models were also characterised in both static and orbital-induced mixing conditions by quantifying ATP and CYP3 A4 production by PHH, in addition to albumin and urea synthesis. With regard to the monoculture models, the characterisation data is summarised in Fig. 4. In particular, ATP production was maintained for 31 days (Fig. 4A), indicating cell viability throughout the entire experiment, with no statistically significant difference between the static and orbital-induced mixing conditions apart from day 11. CYP3 A4 production was also maintained throughout 31 days (Fig. 4B), peaking on day 7 in all conditions, when the CYP3 A4 production was higher in the orbital-induced mixing conditions relative to the static condition. Albumin production (Fig. 4C) was maintained for 26 days in all conditions, peaking on day 7, reaching 40.1 µg/day/10^6 PHH in the orbital-induced mixing condition. With regard to urea production (Fig. 4D), human-relevant levels of urea (> 56 µg/million/PHH/day) [39] were maintained for 7 days in the static condition, decreasing to 24.25 µg by day 14. Conversely, when orbital-induced mixing was introduced into the model, urea production was above the human-level threshold until day 14.

PHH in triculture with liver endothelial cells (LECs) and stellate cells grown on NS were viable throughout the entire experiment in both static and orbital-induced mixing conditions, as evident from the ATP production sustained for 31 days (Fig. 5A). However, in the fluid orbital-induced mixing flow condition, ATP production was elevated compared to the static condition from day 4. Similarly, CYP3 A4 production (Fig. 5B) was also sustained for 31 days. In particular, on day 20, the CYP3 A4 production associated with the orbital-induced mixing flow condition was more than seven times higher than the levels reached in the static condition. The inclusion of NPCs in the triculture model reduces CYP3 A4 activity compared to PHH monocultures.

Albumin production (Fig. 5C) was maintained throughout the entire experiment, and between days 7 and 26, albumin levels in the orbital-induced mixing conditions were markedly higher relative to the static condition. In particular, between days 11 and 26, albumin production in the orbital-induced mixing conditions exceeded the human liver in vivo output threshold of 43 µg/day/10^6 PHH [39]. With regard to urea production (Fig. 5D), values obtained from both conditions were superior to human threshold levels (> 56 µg/million/PHH/day) from days 2 to 14. Additionally, on day 2 in the orbital-induced mixing condition, urea production was markedly higher than the production associated with the static condition.

PHH in tetracultures maintained viability for the entire experiment in both fluid flow and static conditions, as evident from their ATP production (Fig. 6A), which was sustained for 26 days. On day 11, the ATP production associated with the orbital-induced mixing condition was markedly higher than the value associated with the static condition. PHH in tetracultures also maintained CYP3 A4 production at all timepoints (Fig. 6B). In particular, on days 11 and 14, CYP3 A4 levels associated with the orbital-induced mixing condition were higher relative to the static condition. Additionally, on day 11 albumin production was higher in the orbital-induced mixing condition relative to the static condition (Fig. 6C). Albumin production was maintained in both conditions throughout the entire experiment. Urea production in tetraculture displayed a descending trend in both conditions (Fig. 6D) and was consistently above the human level threshold (> 56 µg/million/hepatocytes) for 14 days in both conditions [39]. With regard to Kupffer cells, ATP production was markedly increased in the orbital-induced mixing condition relative to the static condition (Fig. 6E). Kupffer cells did not improve CYP3 A4, ATP, albumin, or urea levels in the tetraculture models.

Overall, the addition of KC to the model did not markedly improve ATP, urea, albumin and CYP3 A4 production relative to the triculture model, whilst the same parameters were increased by the introduction of orbital-induced mixing in all models and across different timepoints. Therefore, triculture and monoculture models inclusive of orbital-induced mixing were used for toxicity screening experiments. In particular, the compounds tested were zileuton (Fig. 7A), buspirone (Fig. 7B), and cyclophosphamide (Fig. 7C), respectively

considered to be most-DILI-concern, ambiguous-DILI-concern and less-DILI-concern drugs by the US FDA [58]. Compounds testing was initiated at timepoints that were found to be associated with ascending trends in CYP3 A4 production according to the results obtained from the characterisation experiment. In particular, the drug dosing protocol began on days 2 and 4 for monocultures and tricultures, respectively. CYP3 A4 is a key enzyme responsible

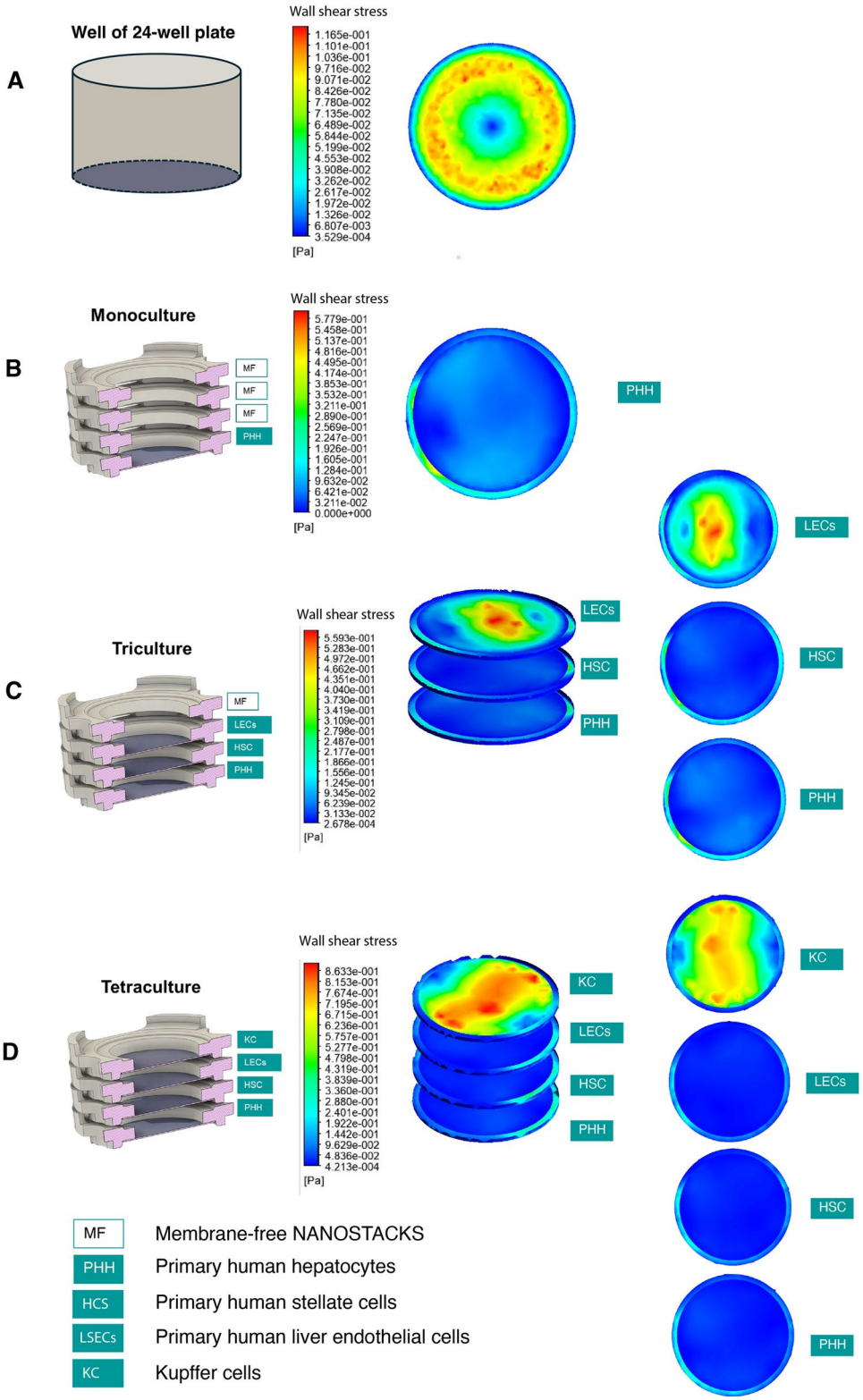

Fig. 3 CFD modelling of shear stress (Pa) induced by an orbital shaker set at 90 rpm, acting on an empty well of a 24-well plate and on NS membranes included in the well. **A** Bottom surface of NS-free well. **B** Membrane of NS placed on bottom of the well, under three membrane-free NS. **C** Membranes of three NS placed on the bottom of the well, under one membrane-free NS. **D** Membranes of four NS placed inside the well

for metabolising a wide range of drugs, including buspirone (major role), cyclophosphamide (moderate), and zileuton (minor), and high CYP expression in PHH in vitro models better mimics human liver metabolism. Each dose of the drug was given every 24 h, and the viability of PHH was analysed after a 7-day period. The IC50/C_{max} of zileuton associated with the triculture was 66.18 mM, which was 1311.3% higher than the monoculture value of 5.047 mM, indicating that NPCs might exert a protective effect on PHH. A similar effect was observed with regard to buspirone, as the IC50/C_{max} associated with tricultures was 31,807 mM, 220.9% higher than the value associated with monocultures (14,402 mM), and with regard to cyclophosphamide, as the IC50/C_{max} associated with tricultures was 367.8 mM, 335.9% higher than the value obtained from monocultures (109.5 mM).

NS-based models can be disassembled, and data can be acquired in relation to each individual NS, as shown in Fig. 7, which depicts the viability of PHH (Fig. 7D), HSC (Fig. 7E), and LECs (Fig. 7F) in the triculture model upon treatment with zileuton, in the static condition. In particular, LECs (IC50/C_{max} = 13.83) were more vulnerable to the toxic effects of zileuton compared to PHH (IC50/C_{max} = 57.1) and HSC (IC50/C_{max} = 99.6).

Discussion

Animal studies encounter significant limitations due to substantial differences in drug metabolism and pharmacokinetics between animals and humans [36, 37]. A recent survey conducted in the pharmaceutical industry shed

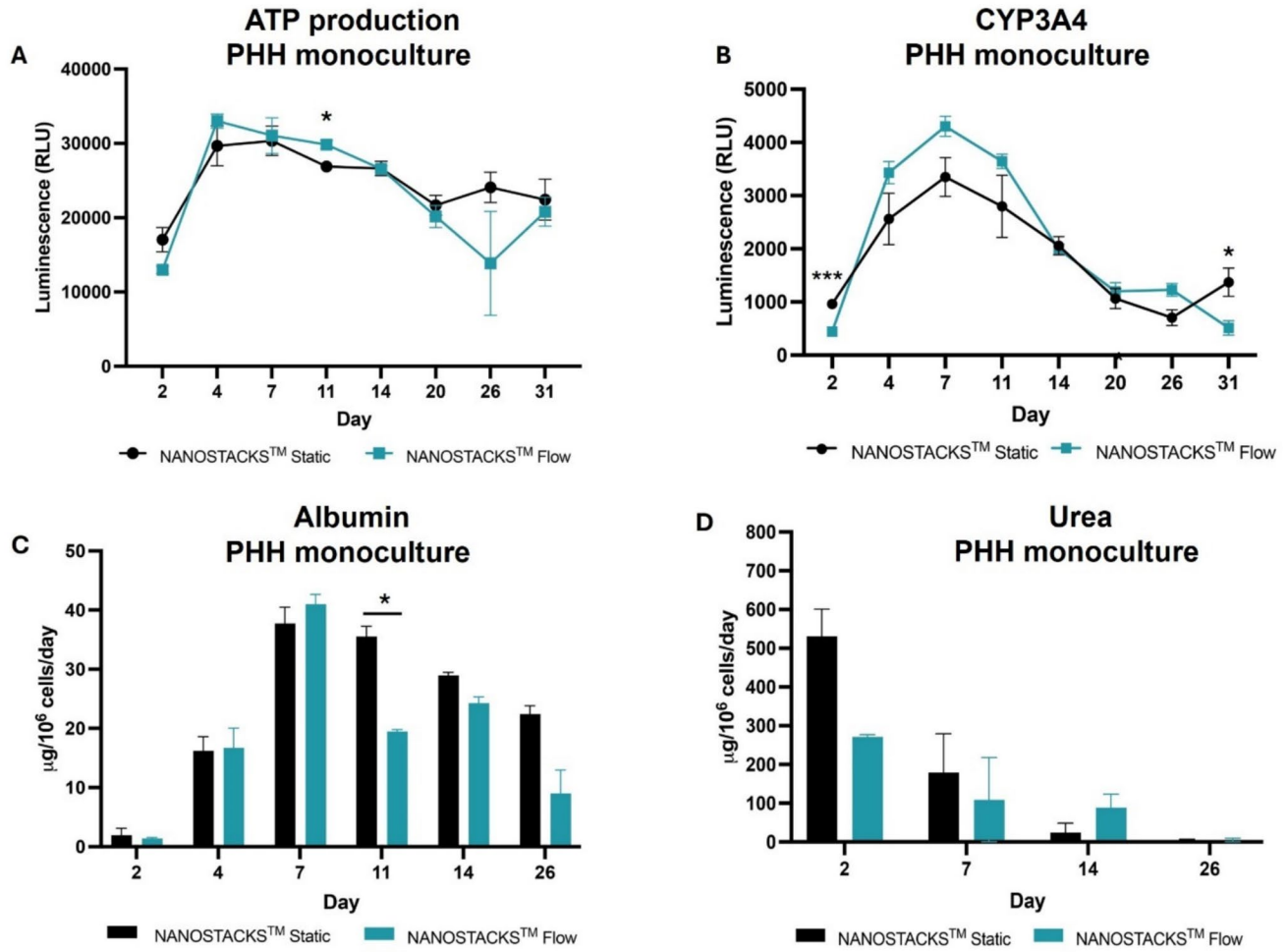

Fig. 4 ATP, CYP3 A4, albumin and urea production from PHH in monocultures in static (black) and orbital-induced mixing flow (blue) conditions. **A** ATP synthesis expressed in relative light units (RLU; *y*-axis) on days 2, 4, 7, 11, 14, 20, 26, and 31 (*x*-axis). **B** CYP3 A4 production, expressed in RLU (*y*-axis), on days 2, 4, 7, 11, 14, 20, 26, and 31 (*x*-axis). **C** Albumin production, expressed in µg/10^6 cells/day (*y*-axis), on days 2, 4, 7, 11, 14, and 26 (*x*-axis). **D** Urea production, expressed in µg/10^6 cells/day (*y*-axis) on days 2, 7, 14, and 26 (*x*-axis). Each datapoint was obtained from n = 3 wells. Data are reported as mean ± SEM

light on the limited concordance between preclinical liver toxicity findings and clinical outcomes [6]. This finding is consistent with prior studies demonstrating the limited predictive capability of preclinical models for human liver toxicity [4]. These studies underscore the limitations of current preclinical testing paradigms in predicting DILI in humans, particularly for compounds with poorly characterised dose–response relationships or unique mechanisms of toxicity. After the US FDA released the Modernization Act 2.0, which allows the use of alternatives to animal testing to investigate the safety and effectiveness of a drug, a need for realistic human in vitro models of the liver for DILI screening has emerged [38]. The main advantages of this approach will be the reduction of both time and costs of drug development, whilst following the principles of the "3 Rs" in relation to the replacement, reduction, and refinement of animal studies in the context of safety and efficacy assessments [39].

In this work, a novel platform called NANOSTACKS™ (NS) was utilised for the assembly of complex hepatic coculture models in a high-throughput 24-well plate format inclusive of orbital-induced mixing. The models included monocultures of PHH, tricultures of PHH, HSC, and LECs, as well as tetracultures comprising PHH, HSC, LECs, and KC. The models were characterised based on parameters associated with hepatic function, both in the absence and presence of orbital-induced mixing. The tricultures and monocultures incorporating orbital-induced mixing were further evaluated for their reliability in the context of DILI screening. This evaluation was conducted using three different compounds to assess the models' effectiveness in predicting hepatic responses.

NS utilised for the development the complex models used in this work include a polycarbonate body and a transparent porous PET membrane, thus using materials that do

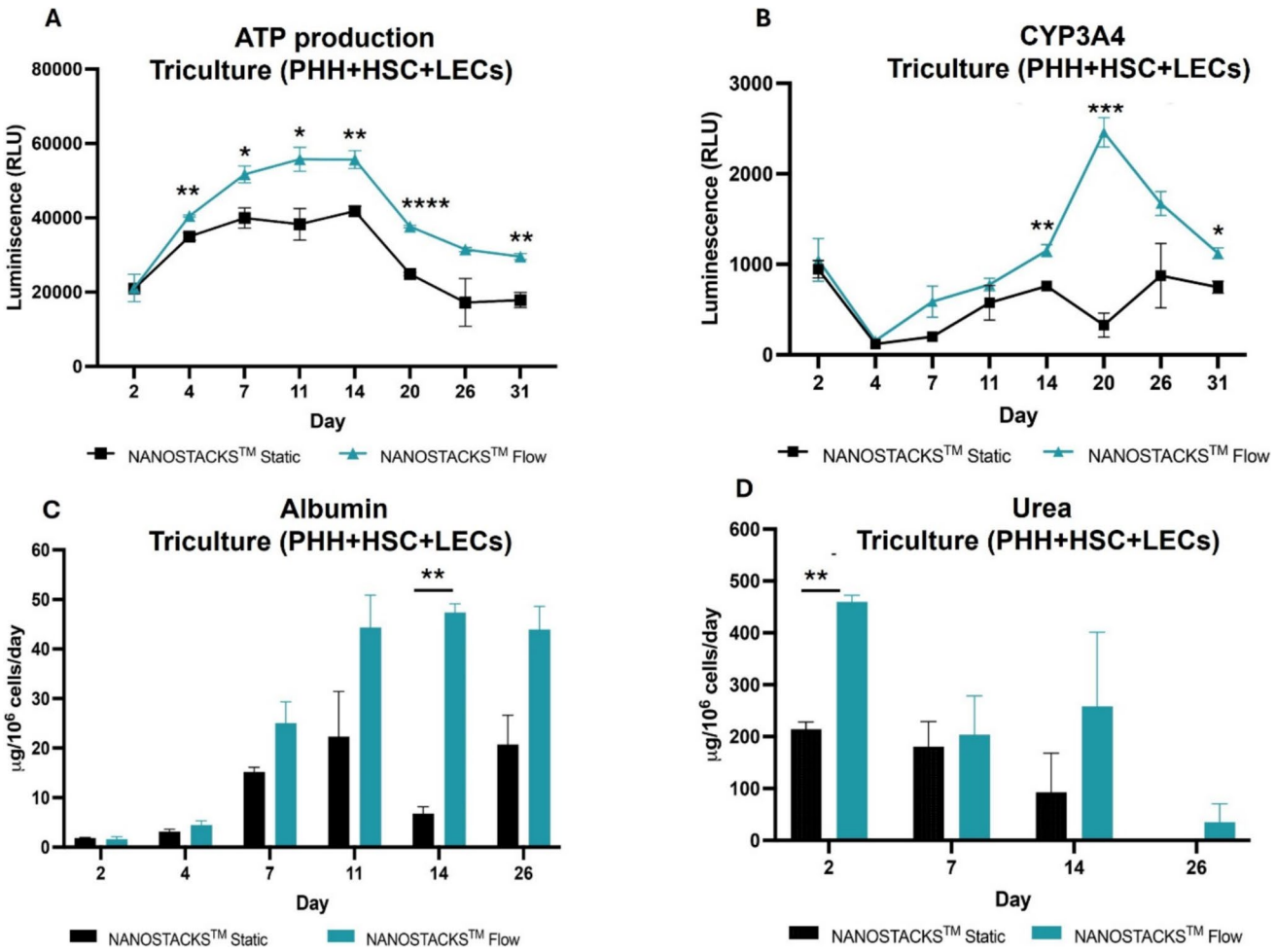

Fig. 5 ATP, CYP3 A4, albumin and urea production from PHH in tricultures in static (black) and orbital-induced mixing flow (blue) conditions. **A** ATP synthesis, expressed in RLU (*y*-axis) on days 2, 4, 7, 11, 14, 20, 26, and 31 (*x*-axis). **B** CYP3 A4 production, expressed in RLU (*y*-axis), on days 2, 4, 7, 11, 14, 20, 26, and 31 (*x*-axis). **C** Albumin production, expressed in µg/10^6 cells/day (*y*-axis), on days 2, 4, 7, 11, 14, and 26 (*x*-axis). **D** Urea production, expressed in µg/10^6 cells/day (*y*-axis) on days 2, 7, 14, and 26 (*x*-axis). Each datapoint was obtained from $n = 3$ wells. Data are reported as mean ± SEM

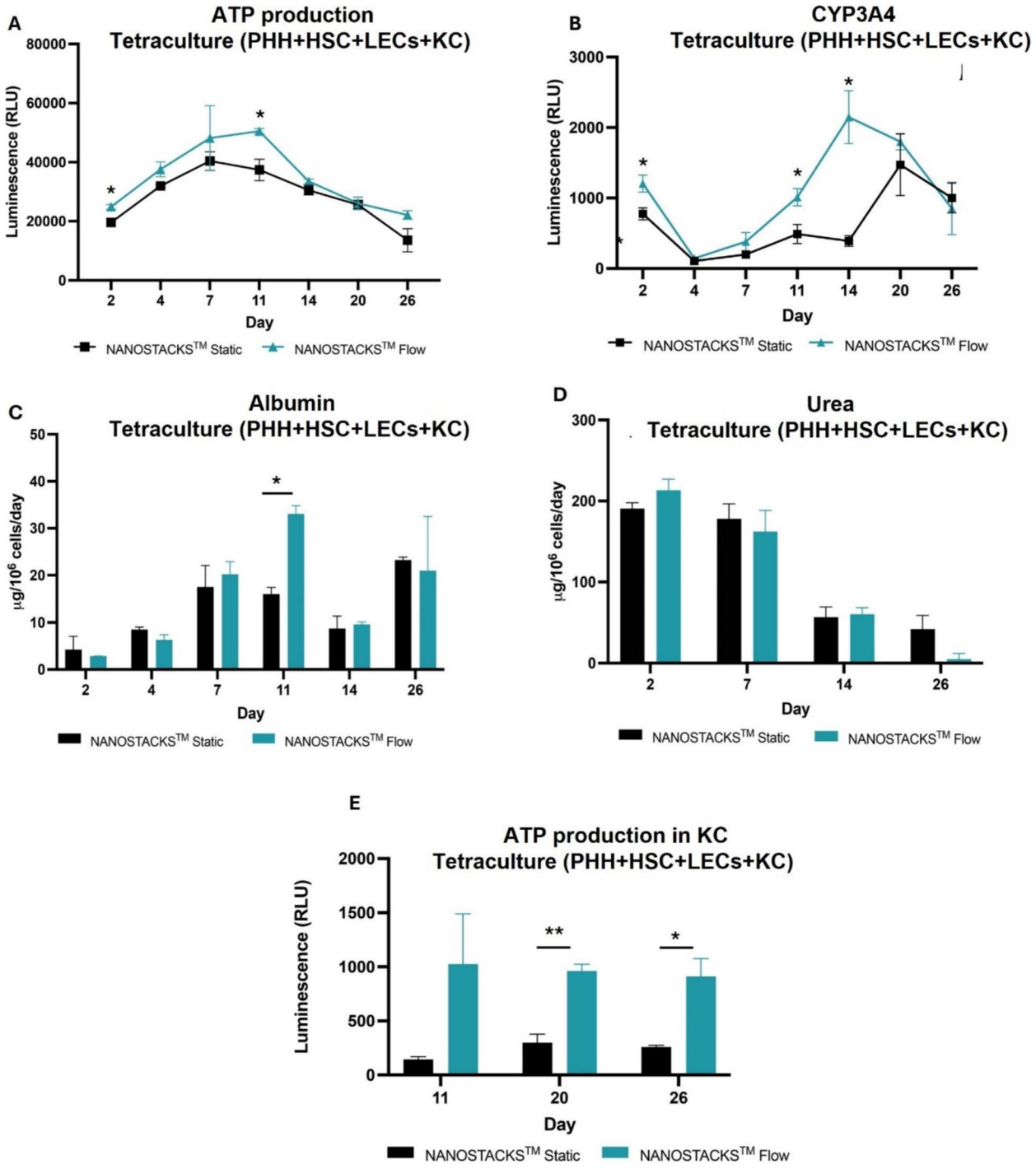

Fig. 6 ATP, CYP3 A4, albumin and urea production from PHH, and ATP synthesis by Kupffer cells in tetracultures, in static (black) and orbital-induced mixing flow (blue) conditions. **A** ATP synthesis by PHH, expressed in RLU (*y*-axis) on days 2, 4, 7, 11, 14, 20, and 26 (*x*-axis). **B** CYP3 A4 production, expressed in RLU (*y*-axis), on days 2, 4, 7, 11, 14, 20, and 26 (*x*-axis). **C** Albumin production, expressed in µg/10^6 cells/day (*y*-axis), on days 2, 4, 7, 11, 14, and 26 (*x*-axis). **D** Urea production, expressed in µg/10^6 cells/day (*y*-axis) on days 2, 7, 14, and 26 (*x*-axis). **E** ATP synthesis by Kupffer cells, expressed in RLU (*y*-axis) on days 11, 20, and 26 (*x*-axis). Each datapoint was obtained from $n = 3$ wells. Data are reported as mean ± SEM

not absorb tested drugs. On the other hand, a considerable number of devices used for the development of complex coculture models are fabricated using polydimethylsiloxane (PDMS), which absorbs a wide spectrum of biochemical compounds, thus altering experimental outcomes of DILI screening [40–42]. Additionally, both drug delivery

challenges and the presence of a necrotic core are associated with the use of spheroids, due to their tightly assembled cellular geometry hampering the diffusion of nutrients and compounds to the innermost cellular layers. Conversely, in vitro models based on NS allow the unobstructed diffusion of compounds and nutrients towards all cellular layers [43]. NS-based models have high reproducibility due to the standardised dimensions of the individual NS. Other features of NS also include optical transparency and the possibility of including orbital-induced mixing in the model. Additionally, NS are compatible with SBS-standard 24-well plates and plate-reader-based assays, in addition to biochemical assays relying on the use of supernatant, thus making NS a user-friendly platform.

In the tricultures and tetracultures models, the ratios of PHH, LECs, HSCs, and KCs are congruent with those associated with native liver tissue [44]. In particular, whilst most coculture models include a NPC : PHH ratio of 1:2 to 1:6 [16, 45, 46], in this study, a 1:3 ratio was used to increase the production of any paracrine signalling molecules associated with NPC.

Cytochrome P450 enzymes (CYPs), including CYP3 A4, are crucial for the first-pass metabolism of xenobiotics. The orbital-induced mixing increased CYP3 A4 production relative to the static condition at multiple timepoints. The CYP3 A4 production observed in all NS-based human liver models was maintained throughout the entire duration of the study, as observed in MPS-based PHH models [47]. Similarly to the results associated with CYP3 A4 production, orbital-induced mixing also increased ATP production on multiple timepoints relative to the static condition.

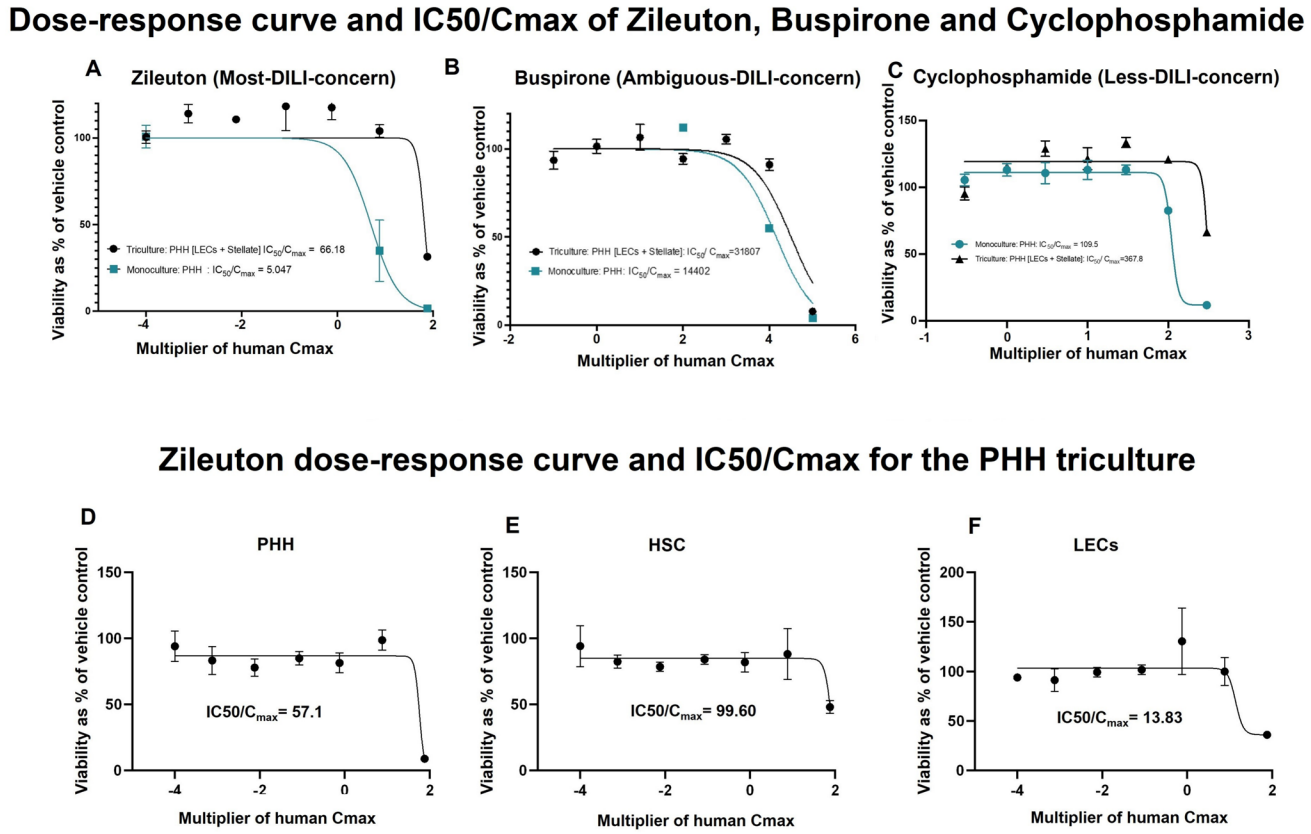

Fig. 7 Toxicity evaluation of zileuton, buspirone, and cyclophosphamide on monoculture and triculture models. Cell viability, reported on the y-axis in all graphs, is expressed as the percentage of ATP production of the vehicle control. Concentrations of the compounds, reported on the x-axis in all graphs, are expressed as multipliers of the human C_{max}. The graphs show data points and dose–response curves obtained by applying a nonlinear regression. **A** PHH viability associated with monoculture (blue) and triculture (black)models inclusive of orbital-induced mixing were treated with Zileuton at concentrations ranging between 0.0001 human C_{max} and 100 human C_{max}. **B** PHH viability associated with monoculture (blue) and triculture (black) models inclusive of orbital-induced mixing were treated with busporine at concentrations ranging between 0.1 human C_{max} and 100,000 human C_{max}. **C** PHH viability associated with monoculture (blue) and triculture (black) models inclusive of orbital-induced mixing were treated with cyclophosphamide at concentrations ranging between 0.3 human C_{max} and 300 human C_{max} (*x*-axis). Cell viability (*y*-axis) of PHH (**D**), HSC (**E**), and LECs (**F**) under static conditions in triculture, treated with zileuton at concentrations ranging between 0.0001 human C_{max} and 100 human C_{max} (*x*-axis). Each data point was obtained from $n = 3$ wells. Data are reported as mean ± SEM

Albumin production was detectable across all three models and was increased by the inclusion of fluid flow in most timepoints. In particular, orbital-induced mixing models, albumin secretion was found to be within the range associated with the in vivo human production rate (37–105 µg per day per 1 million hepatocytes) [39, 48] on day 7 in monocultures, on days 11, 14, and 26 in tricultures, and on day 11 in tetracultures, indicating that these models effectively support hepatocyte functionality. Comparisons can be drawn with regard to other studies. In the work conducted by Tasnim et al., collagen sandwich cultures and spheroids, including rat hepatocytes, have shown relatively higher albumin levels compared to NS-based human-relevant models [49]. However, in the same study, it was noted that rat hepatocytes-derived spheroids had higher albumin production compared to human-derived hepatic spheroids [49], and therefore, the higher production rate associated with rat-derived models as compared to NS-based human models might be due to the hepatocytes origin rather than to the substrate onto which cells are cultured. Nonetheless, despite their albumin production, rat-derived hepatocytes cannot be considered to be as human-relevant as PHH [39]. With regard to studies conducted on human cells, in the study by Rodriguez-Fernandez et al., PHH cultures on a 2D surface did not reach the human in vivo albumin production threshold [50], therefore indicating that PHH cultured on NS might adopt a more human-relevant phenotype as opposed to culture on standard well-plates. However, comparisons with more advanced culture systems, including PHH spheroids, lead to mixed conclusions. In the study conducted by Messner et al., spheroids developed using PHH and liver-derived NPC had higher albumin production rates than NS-based models, over a 5-week period [51]. However, in the study conducted by Esch et al., long-term human liver organoid cultures over 14 days had a lower rate of albumin production compared to NS-based, orbital-induced mixing inclusive models [51]. Mixed results can be obtained with regard to comparisons with MPS-based models, with albumin production being relatively higher or lower than NS-based models depending on factors such as the timepoint, platform, and PHH donor [14, 47, 53].

Urea production in all three NS-based, orbital-induced mixing inclusive models was above the threshold of in vivo human urea production (56–159 µg per day per 1 million hepatocytes) value up to day 7 [39, 54]. Comparatively to the values obtained in the present work, urea production values were lower in models based on rat-derived hepatocytes included in 2D monolayers [54], collagen sandwich cultures [48, 55], spheroid models grown for 7 days [48, 56] and micropatterned coculture of iPSC-derived human hepatocytes cultured for 28 days [31], demonstrating the importance of including human-derived cells in realistic in vitro models [52]. As discussed in relation to albumin production, comparisons with studies analysing the urea production in MPS-based model hold mixed results depending on donor, platform and timepoint [14, 57]. In summary, similarly to MPS platforms, NS-based PHH models inclusive of orbital-induced mixing can replicate human-relevant hepatic markers, such as in vivo albumin production, whilst being user-friendly and fitting into a 24-well plate format [58].

To evaluate the capacity of orbital-induced mixing inclusive, NS-based monoculture and triculture models to be used as a screening platform for DILI, we examined the hepatotoxic effects of zileuton, buspirone, and cyclophosphamide. The PHH included in the triculture model consistently demonstrated greater resistance to cytotoxicity compared to the PHH in monoculture models, particularly in response to zileuton and cyclophosphamide. The enhanced PHH resistance to toxicity effects can be considered an advantageous feature in a DILI screening platform, as it could reduce the incidence of false positives and allow for more accurate estimations of human toxic dosages. Additionally, an advantageous feature of NS-based models is the possibility to analyse separately each NS upon drug testing, in order to assess the cell-specific cytotoxicity of a compound. In this work, this was demonstrated using the drug zileuton and LECs as the first cell type to exhibit injury in response to zileuton. This differential toxicity analysis can be technically challenging in other types of coculture models, such as 2D mixed cocultures and spheroids.

In conclusion, NS can be used for the development of in vitro liver models that are compatible with plate–reader-based assays. Multicellular human liver models developed using NS have shown orbital-induced mixing-dependent increases in the production of ATP, CYP3 A4, albumin, and urea. NS-based models can be used as DILI screening platforms, with PHH in triculture models exhibiting greater resistance to toxicity relative to monocultures. Therefore, NS represents a promising tool for developing complex hepatic in vitro models with a view to reduce the high attrition rate associated with the drug development process. Future work will address the limitations of this research by expanding the donor pool including multiple donors and different cell lots, increasing the number of drugs tested, and evaluating their effects on liver functionality. Tetraculture models will be further characterised and will include incorporating cytokine measurements such as TNF-α and IL-6 and evaluating Kupffer cell activation and applicability for studying immune-mediated DILI. Additionally, NS could also be used for the development of hepatic disease models, such as nonalcoholic steatohepatitis while in silico models integrate in vitro data with machine learning and artificial intelligence, enhancing predictive accuracy.

Acknowledgements We wish to thank Innovate UK for funding this project (Grant: 10035032). NANOSTACKS™ is a patented

technology and consists of a family of patents including UK (Granted: GB1602146), US (Granted: US16/075136), and pending applications in Europe (EP1713365.9) and under the WIPO (PCT/GB2017/090286).

Author contributions A.T. and R.S. undertook experimental work, helped construct figures and prepare an initial draft manuscript; V.H., T.J. and A.R. undertook data analyses and helped construct figures; I.I.P. and F.L.M. gave advice on experimental set-up and study design; and, V.L. was the Principal Investigator, led the project and acquired funding for the project. All authors reviewed the final manuscript.

Funding We wish to thank Innovate UK for funding this project (Grant number: 10035032).

Data availability No datasets were generated or analysed during the current study.

Declarations

Competing interests This technology has emerged from R&D in a SME, Revivocell Ltd. The SME is looking in the future towards commercialisation of the patented technology described herein.

References

1. Andrade RJ, Chalasani N, Björnsson ES, Suzuki A, Kullak-Ublick GA, Watkins PB, Devarbhavi H, Merz M, Lucena MI, Kaplowitz N, Aithal GP. Drug-induced liver injury. Nat Rev Dis Prim. 2019;5(1):58.
2. Watkins PB. Drug safety sciences and the bottleneck in drug development. Clin Pharmacol Ther. 2011;89(6):788–90.
3. Hornberg JJ, Laursen M, Brenden N, Persson M, Thougaard AV, Toft DB, Mow T. Exploratory toxicology as an integrated part of drug discovery Part I: why and how. Drug Discov Today. 2014;19(8):1131–6.
4. Olson H, Betton G, Robinson D, Thomas K, Monro A, Kolaja G, Lilly P, Sanders J, Sipes G, Bracken W, Dorato M. Concordance of the toxicity of pharmaceuticals in humans and in animals. Regul Toxic Pharmacol. 2000;32(1):56–67.
5. McGill MR, Jaeschke H. 2019 Animal models of drug-induced liver injury. Biochim Biophys Acta (BBA)-Mol Basis Dis. 1865(5):1031-9
6. Monticello TM, Jones TW, Dambach DM, Potter DM, Bolt MW, Liu M, Keller DA, Hart TK, Kadambi VJ. Current nonclinical testing paradigm enables safe entry to First-In-Human clinical trials: the IQ consortium nonclinical to clinical translational database. Toxicol Appl Pharmacol. 2017;1(334):100–9.
7. Serras AS, Rodrigues JS, Cipriano M, Rodrigues AV, Oliveira NG, Miranda JP. A critical perspective on 3D liver models for drug metabolism and toxicology studies. Front Cell Dev Biol. 2021;22(9):626805.
8. Han JJ. FDA Modernization Act 2.0 allows for alternatives to animal testing
9. Collins SD, Yuen G, Tu T, Budzinska MA, Spring KJ, Bryant K, Shackel NA. In vitro models of the liver: disease modeling, drug discovery and clinical applications. Hepatocellular carcinoma. 2019:47-67
10. Underhill GH, Khetani SR. Bioengineered liver models for drug testing and cell differentiation studies. Cell Mol Gastroenterol Hepatol. 2018;5(3):426–39.
11. Proctor WR, Foster AJ, Vogt J, Summers C, Middleton B, Pilling MA, Shienson D, Kijanska M, Ströbel S, Kelm JM, Morgan P. Utility of spherical human liver microtissues for prediction of clinical drug-induced liver injury. Arch Toxicol. 2017;91:2849–63.
12. Takebe T, Sekine K, Enomura M, Koike H, Kimura M, Ogaeri T, Zhang RR, Ueno Y, Zheng YW, Koike N, Aoyama S. Vascularized and functional human liver from an iPSC-derived organ bud transplant. Nature. 2013;499(7459):481–4.
13. Palma E, Doornebal EJ, Chokshi S. Precision-cut liver slices: a versatile tool to advance liver research. Hepatol Int. 2019;15(13):51–7.
14. Ewart L, Apostolou A, Briggs SA, Carman CV, Chaff JT, Heng AR, Jadalannagari S, Janardhanan J, Jang KJ, Joshipura SR, Kadam MM. Qualifying a human liver-chip for predictive toxicology: performance assessment and economic implications. Biorxiv. 2021;16:2021–12.
15. Borgström A, Filippi BG, Hewitt P, Wolf A, Gebauer M. Expression analysis of exosomal microRNAs in chlorpromazine treated human hepatic spheroids: a promising tool for novel drug-induced liver injury biomarker discovery. Appl In Vitro Toxicol. 2023;9(2):65–76.
16. Bell CC, Chouhan B, Andersson LC, Andersson H, Dear JW, Williams DP, Söderberg M. Functionality of primary hepatic non-parenchymal cells in a 3D spheroid model and contribution to acetaminophen hepatotoxicity. Arch Toxicol. 2020;94:1251–63.
17. LeCluyse EL. Human hepatocyte culture systems for the in vitro evaluation of cytochrome P450 expression and regulation. Eur J Pharm Sci. 2001;13(4):343–68.
18. Bell CC, Dankers AC, Lauschke VM, Sison-Young R, Jenkins R, Rowe C, Goldring CE, Park K, Regan SL, Walker T, Schofield C. Comparison of hepatic 2D sandwich cultures and 3D spheroids for long-term toxicity applications: a multicenter study. Toxicol Sci. 2018;162(2):655–66.
19. Dash A, Inman W, Hoffmaster K, Sevidal S, Kelly J, Obach RS, Griffith LG, Tannenbaum SR. Liver tissue engineering in the evaluation of drug safety. Expert Opin Drug Metab Toxicol. 2009;5(10):1159–74.
20. Uyama N, Shimahara Y, Kawada N, Seki S, Okuyama H, Iimuro Y, Yamaoka Y. Regulation of cultured rat hepatocyte proliferation by stellate cells. J Hepatol. 2002;36(5):590–9.
21. Thomas RJ, Bhandari R, Barrett DA, Bennett AJ, Fry JR, Powe D, Thomson BJ, Shakesheff KM. The effect of three-dimensional coculture of hepatocytes and hepatic stellate cells on key hepatocyte functions in vitro. Cells Tissues Organs. 2006;181(2):67–79.
22. Kidambi S, Sheng L, Yarmush ML, Toner M, Lee I, Chan C. Patterned co-culture of primary hepatocytes and fibroblasts using polyelectrolyte multilayer templates. Macromol Biosci. 2007;7(3):344–53.
23. Domansky K, Inman W, Serdy J, Dash A, Lim MH, Griffith LG. Perfused multiwell plate for 3D liver tissue engineering. Lab Chip. 2010;10(1):51–8.
24. Chia SM, Lin PC, Yu H. TGF-β1 regulation in hepatocyte-NIH3T3 co-culture is important for the enhanced hepatocyte function in 3D microenvironment. Biotechnol Bioeng. 2005;89(5):565–73.
25. Bhandari RN, Riccalton LA, Lewis AL, Fry JR, Hammond AH, Tendler SJ, Shakesheff KM. Liver tissue engineering: a role for co-culture systems in modifying hepatocyte function and viability. Tissue Eng. 2001;7(3):345–57.
26. Ohno M, Motojima K, Okano T, Taniguchi A. Up-regulation of drug-metabolizing enzyme genes in layered co-culture of a human liver cell line and endothelial cells. Tissue Eng Part A. 2008;14(11):1861–9.
27. Chiew GG, Fu A, Perng Low K, Qian Luo K. Physical supports from liver cancer cells are essential for differentiation and remodeling of endothelial cells in a HepG2-HUVEC co-culture model. Sci Rep. 2015;5(1):10801.

28. Zinchenko YS, Schrum LW, Clemens M, Coger RN. Hepatocyte and kupffer cells co-cultured on micropatterned surfaces to optimize hepatocyte function. Tissue Eng. 2006;12(4):751–61.
29. Li F, Cao L, Parikh S, Zuo R. Three-dimensional spheroids with primary human liver cells and differential roles of Kupffer cells in drug-induced liver injury. J Pharm Sci. 2020;109(6):1912–23.
30. Han B, Mo H, Svarovskaia E, Mateo R. A primary human hepatocyte/hepatic stellate cell co-culture system for improved in vitro HBV replication. Virology. 2021;1(559):40–5.
31. Ware BR, Berger DR, Khetani SR. Prediction of drug-induced liver injury in micropatterned co-cultures containing iPSC-derived human hepatocytes. Toxicol Sci. 2015;145(2):252–62.
32. Chatterjee S, Richert L, Augustijns P, Annaert P. Hepatocyte-based in vitro model for assessment of drug-induced cholestasis. Toxicol Appl Pharm. 2014;274(1):124–36.
33. Deharde D, Schneider C, Hiller T, Fischer N, Kegel V, Lübberstedt M, Freyer N, Hengstler JG, Andersson TB, Seehofer D, Pratschke J. Bile canaliculi formation and biliary transport in 3D sandwich-cultured hepatocytes in dependence of the extracellular matrix composition. Arch Toxicol. 2016;90:2497–511.
34. Saxton SH, Stevens KR. 2D and 3D liver models. J Hepatol. 2023;78(4):873–5.
35. Driessen R, Zhao F, Hofmann S, Bouten C, Sahlgren C, Stassen O. Computational characterization of the dish-in-a-dish a high yield culture platform for endothelial shear stress studies on the orbital shaker. Micromachines. 2020;11(6):552.
36. Lewis DF, Ioannides C, Parke DV. Cytochromes P450 and species differences in xenobiotic metabolism and activation of carcinogen. Environ Health Perspect. 1998;106(10):633–41.
37. Peter JO, Chan K, Silber PM. Human and animal hepatocytes in vitro with extrapolation in vivo. Chemico-Biol Interact. 2004;150(1):97–114.
38. Adashi EY, O'Mahony DP, Cohen IG. The FDA modernization Act 2.0: drug testing in animals is rendered optional. Am J Med. 2023;136(9):853–4.
39. Baudy AR, Otieno MA, Hewitt P, Gan J, Roth A, Keller D, Sura R, Van Vleet TR, Proctor WR. Liver microphysiological systems development guidelines for safety risk assessment in the pharmaceutical industry. Lab on a Chip. 2020;20(2):215–25.
40. Ma LD, Wang YT, Wang JR, Wu JL, Meng XS, Hu P, Mu X, Liang QL, Luo GA. Design and fabrication of a liver-on-a-chip platform for convenient, highly efficient, and safe in situ perfusion culture of 3D hepatic spheroids. Lab on a Chip. 2018;18(17):2547–62.
41. Carius P, Weinelt FA, Cantow C, Holstein M, Teitelbaum AM, Cui Y. Addressing the ADME challenges of compound loss in a PDMS-based gut-on-chip microphysiological system. Pharmaceutics. 2024;16(3):296.
42. Van Meer BJ, de Vries H, Firth KS, van Weerd J, Tertoolen LG, Karperien HB, Jonkheijm P, Denning C, IJzerman AP, Mummery CL. Small molecule absorption by PDMS in the context of drug response bioassays. Biochem Biophys Res Commun. 2017;482(2):323–8.
43. Mehta G, Hsiao AY, Ingram M, Luker GD, Takayama S. Opportunities and challenges for use of tumor spheroids as models to test drug delivery and efficacy. J Control Release. 2012;164(2):192–204.
44. Zeilinger K, Freyer N, Damm G, Seehofer D, Knöspel F. Cell sources for in vitro human liver cell culture models. Exp Biol Med. 2016;241(15):1684–98.
45. Hurrell T, Kastrinou-Lampou V, Fardellas A, Hendriks DF, Nordling Å, Johansson I, Baze A, Parmentier C, Richert L, Ingelman-Sundberg M. Human liver spheroids as a model to study aetiology and treatment of hepatic fibrosis. Cells. 2020;9(4):964.
46. Ware BR, Durham MJ, Monckton CP, Khetani SR. A cell culture platform to maintain long-term phenotype of primary human hepatocytes and endothelial cells. Cell Mol Gastroenterol Hepatol. 2018;5(3):187–207.
47. Rubiano A, Indapurkar A, Yokosawa R, Miedzik A, Rosenzweig B, Arefin A, Moulin CM, Dame K, Hartman N, Volpe DA, Matta MK. Characterizing the reproducibility in using a liver microphysiological system for assaying drug toxicity metabolism, and accumulation. Clin Transl Sci. 2021;14(3):1049–61.
48. Ballmer PE, McNurlan MA, Milne E, Heys SD, Buchan V, Calder AG, Garlick PJ. Measurement of albumin synthesis in humans: a new approach employing stable isotopes. Am J Phys-Endocrinol Metab. 1990;259(6):E797-803.
49. Tasnim F, Singh NH, Tan EK, Xing J, Li H, Hissette S, Manesh S, Fulwood J, Gupta K, Ng CW, Xu S. Tethered primary hepatocyte spheroids on polystyrene multi-well plates for high-throughput drug safety testing. Sci Rep. 2020;10(1):4768.
50. Rodriguez-Fernandez J, Garcia-Legler E, Villanueva-Badenas E, Donato MT, Gomez-Ribelles JL, Salmeron-Sanchez M, Gallego-Ferrer G, Tolosa L. Primary human hepatocytes-laden scaffolds for the treatment of acute liver failure. Biomater Adv. 2023;1(153):213576.
51. Messner S, Agarkova I, Moritz W, Kelm JM. Multi-cell type human liver microtissues for hepatotoxicity testing. Arch Toxicol. 2013;87(1):209–13.
52. Esch MB, Prot JM, Wang YI, Miller P, Llamas-Vidales JR, Naughton BA, Applegate DR, Shuler ML. Multi-cellular 3D human primary liver cell culture elevates metabolic activity under fluidic flow. Lab on a Chip. 2015;15(10):2269–77.
53. Török E, Lutgehetmann M, Bierwolf J, Melbeck S, Düllmann J, Nashan B, Ma PX, Pollok JM. Primary human hepatocytes on biodegradable poly (l-lactic acid) matrices: a promising model for improving transplantation efficiency with tissue engineering. Liver Transplant. 2011;17(2):104–14.
54. Rudman D, DiFulco TJ, Galambos JT, Smith RB, Salam AA, Warren WD. Maximal rates of excretion and synthesis of urea in normal and cirrhotic subjects. J Clin Investig. 1973;52(9):2241–9.
55. Bale SS, Golberg I, Jindal R, McCarty WJ, Luitje M, Hegde M, Bhushan A, Usta OB, Yarmush ML. Long-term coculture strategies for primary hepatocytes and liver sinusoidal endothelial cells. Tissue Eng Part C Methods. 2015;21(4):413–22.
56. Kim MK, Jeong W, Jeon S, Kang HW. 3D bioprinting of dECM-incorporated hepatocyte spheroid for simultaneous promotion of cell-cell and-ECM interactions. Front Bioeng Biotechnol. 2023;13(11):1305023.
57. Xiao RR, Lv T, Tu X, Li P, Wang T, Dong H, Tu P, Ai X. An integrated biomimetic array chip for establishment of collagen-based 3D primary human hepatocyte model for prediction of clinical drug-induced liver injury. Biotechnol Bioeng. 2021;118(12):4687–98.
58. Chen M, Suzuki A, Thakkar S, Yu K, Hu C, Tong W. DILIrank: the largest reference drug list ranked by the risk for developing drug-induced liver injury in humans. Drug Discov Today. 2016;21(4):648–53.